Science and Technology Indonesia
e-ISSN:2580-4391 *p*-ISSN:2580-4405
Vol. 11, No. 3, July 2026

Research Paper

Adsorption of Malachite Green Dye onto Bagasse Ash-Based Silica Aerogel/MgO Composite: Kinetic, Isotherm, and Thermodynamic Studies

Nazriati[1*], Istighfarin Meilidya Azhar[1], Irma Kartika Kusumaningrum[1]

[1]*Department of Chemistry, Faculty of Mathematics and Natural Sciences, Universitas Negeri Malang, Malang, East Java, 65145, Indonesia*
***Corresponding author**: nazriati.fmipa@um.ac.id*

Abstract
A silica aerogel/MgO composite synthesized from bagasse ash was investigated as a biomass-derived adsorbent for the removal of malachite green from aqueous solutions. The adsorption performance was systematically assessed by examining operational factors together with adsorption kinetics, equilibrium isotherms, and thermodynamic behavior. Equilibrium was attained after 80 min of contact time. Under the optimum conditions, the composite achieved an adsorption capacity of 123.19 mg/g at 45°C with an initial concentration of 55 mg/L, while the highest removal efficiency (90.93%) was obtained at pH 9. Comparative experiments demonstrated the superior adsorption capability of the silica aerogel/MgO composite relative to pristine silica aerogel. Adsorption capacities of 96.93 and 22.12 mg/g, respectively, were recorded under the same experimental conditions, highlighting the beneficial interaction between porous silica framework and MgO active sites. Analysis of adsorption kinetic revealed that the pseudo-second-order model most accurately represented the experimental data, yielding an R^2 value of 0.9923. Equilibrium studies further indicated that the Freundlich isotherm provided the best fit ($R^2 = 0.9965$–0.9973), suggesting adsorption on energetically heterogeneous surfaces with the possibility of multilayer uptake. Thermodynamic evaluation confirmed that the adsorption process occurred spontaneously and was favored at elevated temperatures. This behavior was evidenced by negative Gibbs free energy values ($\Delta G^\circ = -4.68$ to -6.29 kJ/mol), positive enthalpy changes ($\Delta H^\circ = 12.46$–15.29 kJ/mol), and positive entropy values ($\Delta S^\circ = 58.76$–67.10 J/mol·K. Overall, the results demonstrate the strong potential of the bagasse ash-derived silica aerogel/MgO composite as an efficient and sustainable adsorbent for the removal of cationic dyes from water.

Keywords
Silica Aerogel/MgO Composite, Malachite Green, Adsorption

Received: 24 February 2026, Accepted: 18 June 2026
https://doi.org/10.26554/sti.2026.11.3.1241-1256

1. INTRODUCTION

The textile industry is widely known for its intensive water usage and for generating substantial volumes of wastewater contaminated with synthetic dyes, largely as a result of dyeing and finishing processes (Tarekegn et al., 2021). The synthetic colorant widely applied in the textile industry is malachite green, which belongs to the triphenylmethane dye group. This substance is characterized by pronounced toxicity, potential carcinogenic effects, limited biodegradability, and a tendency to accumulate within aquatic biota in its reduced form, leucomalachite green (Abu Elella et al., 2021; Umeh et al., 2023; Akram et al., 2023). If not properly treated, this effluent can contaminate aquatic environments and pose serious risks to aquatic organisms. Therefore, effective wastewater treatment methods are required to remove this dye from aquatic environments.

Various methods have been investigated for dye removal, including membrane filtration, catalytic treatment, coagulation, photocatalysis, and adsorption (Raval et al., 2016; Pandey et al., 2020; Agustina et al., 2022). Among the available techniques, adsorption is frequently regarded as a highly effective option because it offers simple operational procedures, adaptable processing conditions, and comparatively economical implementation (Foo and Hameed, 2010). Silica aerogel-based adsorbents are particularly interesting because their interconnected porous framework, extensive specific surface area, and substantial pore volume, all of which enhance the mass transfer and diffusion of adsorbate molecules. Silica aerogel derived from bagasse ash represents an environmentally friendly and value-added alternative adsorbent; however, its surface interaction with cationic dyes remains limited. To enhance adsorption performance, silica aerogel can be composited with magnesium oxide (MgO), which possesses basic and polar surface characteristics that enable electrostatic interactions with positively charged groups in cationic dye molecules such as malachite green (Gui et al.,

2015; Wang et al., 2023). Mechanistically, MgO contributes basic active sites that promote electrostatic attraction and surface interaction, while the silica aerogel framework provides porous channels that support mass transfer and MgO dispersion. This combination is expected to improve the accessibility, distribution, and stability of adsorption sites.

A number of investigations have demonstrated the use of materials derived from MgO and silica as effective adsorbents for removing cationic dyes. However, several critical limitations remain. Studies employing MgO as a single adsorbent often report strong interactions with cationic dyes but are limited by relatively low surface area and structural stability, whereas silica-based adsorbents exhibit high surface area but weaker interactions with cationic species. Furthermore, most investigations primarily focus on adsorption capacity or the influence of a single operational parameter, without critically comparing adsorption performance and modeling outcomes (kinetics, isotherm, and thermodynamics) across different systems. Consequently, systematic studies that comprehensively correlate operational adsorption parameters with adsorption equilibrium behavior remain relatively limited (Benjelloun et al., 2021; Murphy et al., 2023; Shoaib et al., 2023; Liu et al., 2023). This limitation reduces the ability to fully interpret adsorption mechanisms and hinders the rational design of high-performance adsorbents.

Moreover, although composite systems have been reported, studies that explicitly investigate the synergistic interaction between MgO active sites and the porous structure of silica aerogel, particularly those derived from biomass waste such as bagasse ash, are still scarce (Nazriati et al., 2014). Therefore, a comprehensive study integrating operational parameters with adsorption equilibrium modeling for malachite green removal using bagasse ash-derived silica aerogel/MgO composites has not been thoroughly reported.

In this study, bagasse ash-derived silica aerogel modified with MgO was applied for malachite green adsorption from aqueous solution. This work aims to address the limitations of previous studies by integrating operational adsorption parameters with equilibrium modeling in a single systematic framework. Specifically, the objectives of this study are to: (1) evaluate the influence of contact time, adsorbent dosage, initial dye concentration, temperature, and solution pH on adsorption performance; and (2) comprehensively analyze adsorption behavior through kinetic, isotherm, and thermodynamic analyses to clarify the adsorption behavior.

The main contribution of this work lies in (i) providing a comprehensive understanding of adsorption mechanisms through integrated analysis, (ii) demonstrating the synergistic interaction between MgO active sites and silica aerogel porous structure, and (iii) introducing a sustainable adsorbent derived from biomass waste (bagasse ash) with enhanced adsorption performance.

2. EXPERIMENTAL SECTION

2.1 Materials and Instrumentation

In this work, a silica aerogel/MgO composite derived from bagasse ash was employed as the adsorbent material. The materials used in this research included bagasse ash, sodium hydroxide (NaOH, p.a., Merck), magnesium chloride hexahydrate ($MgCl_2{\cdot}6H_2O$, p.a., Merck), ammonium hydroxide (NH_4OH, 25%, Merck), malachite green (p.a., Merck), hydrochloric acid (HCl, 37%, Merck), and distilled water. The instrumentation used in this study was XRD (PANalytical X'Pert PRO), Specific Surface Area and Pore Analysis (Micromeritics Tristar II Plus 3.04), FTIR (Bruker Alpha instrument), SEM (FEI Inspect-S50), and UV-Vis (B-ONE UV-1800).

2.2 Methods

2.2.1 Synthesis of Silica Aerogel/MgO Composite

The silica aerogel/MgO composite was prepared using an adapt ed procedure derived from Azhar et al. Azhar et al. (2025), with several modifications introduced to enhance MgO dispersion and improve the structural robustness of the resulting composite. Initially, 3 g of $MgCl_2{\cdot}6H_2O$ was dissolved in 300 mL of distilled water contained in a 500 mL beaker. Subsequently, 10 mL of 3 M NH_3 solution was introduced into the mixture, which was then maintained under magnetic stirring at 300 rpm for 30 min to promote complete dissolution and uniform distribution of the magnesium precursor. Following the preparation of the precursor solution, 1 g of silica aerogel (procedure adapted from Nazriati et al. (2014) was gradually incorporated into the suspension. The mixture was continuously agitated at room temperature for 24 h to facilitate the diffusion and incorporation of magnesium species within the porous silica aerogel structure. To further strengthen the interaction between the magnesium precursor and the silica framework, the suspension was subsequently left undisturbed for an additional 24 h. After the aging stage, the solid material was recovered by filtration and repeatedly rinsed with distilled water until the filtrate reached neutral pH, thereby eliminating residual ionic species. The recovered solid was then subjected to drying at 80°C for 2 h to remove physically retained moisture. Thermal treatment was carried out in two steps: an initial calcination at 300°C for 1 h, followed by second calcination at 525°C for 2.5 h. These heat-treatment stages enabled the transformation of the magnesium precursor into MgO while simultaneously improving the crystallinity, stability, and dispersion of MgO particles throughout the silica aerogel matrix. The modifications applied in this synthesis route were intended to maximize the interaction between MgO and porous silica network and to achieve a more homogeneous composite structure.

2.2.2 Adsorption Procedure

Batch adsorption experiments were carried out by contacting a fixed volume (25 mL) of malachite green solution with the adsorbent in 50 mL Erlenmeyer flask. The mixtures were maintained under continuous shaking at 150 rpm throughout the adsorption period. After equilibration, the suspensions

were centrifuged at 1500 rpm for 15 min, and residual dye concentration in the liquid phase was determined spectrophotometrically using UV-Vis instrument.

The effect of several operating parameters were systematically evaluated. Adsorption time varied between 30 and 120 min, whereas adsorbent dosage range from 5 to 50 mg. To assess the influence of initial dye concentration, malachite green solutions with concentration 35–55 mg/L were employed. Temperature studies were performed at 25, 35, and 45°C, and solution pH was adjusted within the range of 3–9 using 0.05 M NaOH.

2.2.3 Determination of the pH_{PZC} (pH at the Point of Zero Charge)

The point of zero charge (pH_{PZC}) of the adsorbent was determined using the pH drift method to establish the pH at which the surface possesses no net electrical charge. Briefly, 0.025 g of adsorbent was dispersed in 25 mL of 0.1 M NaCl solution. The initial pH of the suspensions was adjusted over a range of 2–12 using either 1 M HCl or 1 M NaOH. The resulting mixtures maintained under continuous stirring for 24 h to allow the system to reach equilibrium. Following equilibration, the final pH values were measured and compared with their corresponding initial pH values. The difference between these values ($\Delta pH = pH_f - pH_i$) was calculated and plotted as a function of the initial pH. The pH_{PZC} was subsequently identified from the intersection point where the ΔpH value became zero.

2.2.4 Reusability Test

The reusability test was performed to evaluate whether the adsorbent could be regenerated for repeated use. Malachite green adsorption was first performed using 0.01 g of silica aerogel/MgO in 50 mg/L dye solution. After adsorption, the spent adsorbent was separated and immersed in 0.1 M NaCl at 45°C to release the adsorbed dye. The material was then rinsed with deionized water, dried at 100°C, and used again in the next adsorption cycle.

2.2.5 Adsorption Data Analysis

The adsorption performance was quantified by calculating the uptake capacity and removal efficiency based on concentration changes before and after treatment. Kinetic modeling was interpreted using pseudo-first-order and pseudo-second-order equations, while equilibrium behavior was analyzed via the Langmuir, Freundlich, and Temkin isotherms. Thermodynamic parameters were derived to determine the feasibility and energetic characteristics of the adsorption process.

The adsorption capacity at equilibrium (q_e) was determined using Equation (1), whereas the removal efficiency (R, %) of malachite green was calculated using Equation (2).

$$q_e = \frac{(C_0 - C_e)V}{m} \tag{1}$$

$$R(\%) = \frac{C_0 - C_e}{C_0} \times 100 \tag{2}$$

In Equations (1) and (2), C_0 and C_e (mg/L) denote the initial and equilibrium concentrations of malachite green, respectively, V (L) represents the solution volume, and m (g) refers to the mass of adsorbent used in the experiment.

2.2.5.1 Kinetic Models

The pseudo-first-order and pseudo-second-order kinetic models are expressed in Equations (3) and (4):

a. Pseudo-first-order

$$\ln(q_e - q_t) = \ln q_e - k_1 t \tag{3}$$

b. Pseudo-second-order

$$\frac{t}{q_t} = \frac{1}{k_2 q_e^2} + \frac{t}{q_e} \tag{4}$$

k_1 (min^{-1}) and k_2 (g mg^{-1} min^{-1}) represent the rate constants of the pseudo-first-order and pseudo-second-order kinetic models, respectively.

2.2.5.2 Isotherm Models

The Langmuir, Freundlich, and Temkin models are represented in Equations (5)–(7):

a. Langmuir

$$q_e = \frac{q_{max} K_L C_e}{1 + K_L C_e} \tag{5}$$

b. Freundlich

$$q_e = K_F C_e^{1/n} \tag{6}$$

c. Temkin

$$q_e = B_T \ln A_T + B_T \ln C_e \tag{7}$$

The physical meanings of the isotherm parameters are summarized in Table 1.

2.2.5.3 Thermodynamic Parameters

The thermodynamic values were calculated using Equations (8)–(10):

$$K_c = \frac{q_e}{C_e} \tag{8}$$

$$\Delta G^\circ = -RT \ln K_c \tag{9}$$

$$\ln K_c = \frac{\Delta S^\circ}{R} - \frac{\Delta H^\circ}{RT} \tag{10}$$

K_c is the equilibrium constant. R (8.314 J/mol·K) is the gas constant, and T (K) is the absolute temperature. The parameters ΔG°, ΔH°, and ΔS° describe Gibbs free energy (kJ/mol), enthalpy (kJ/mol), and entropy (J/mol·K), respectively.

Table 1. Parameters and Physical Meaning of Adsorption Isotherm

Model	Parameter	Unit	Physical Meaning
Langmuir	q_{max}	mg g^{-1}	Theoretical maximum adsorption capacity
Langmuir	K_L	L mg^{-1}	Langmuir affinity constant
Freundlich	K_F	(mg g^{-1})(L $mg^{-1})^{1/n}$	Indicator of adsorption capacity on heterogeneous surfaces
Freundlich	$1/n$	–	Heterogeneous factor
Temkin	A_T	L g^{-1}	Temkin equilibrium binding constant
Temkin	B_T	J mol^{-1}	Constant related the variation of adsorption energy or heat of adsorption
	$B_T = RT/b_T$		
Temkin	b_T	J mol^{-1}	Temkin adsorption constant used in the calculation of BT

3. RESULTS AND DISCUSSION

3.1 Characterization of Silica Aerogel/MgO Composites

3.1.1 XRD (X-ray Diffraction)

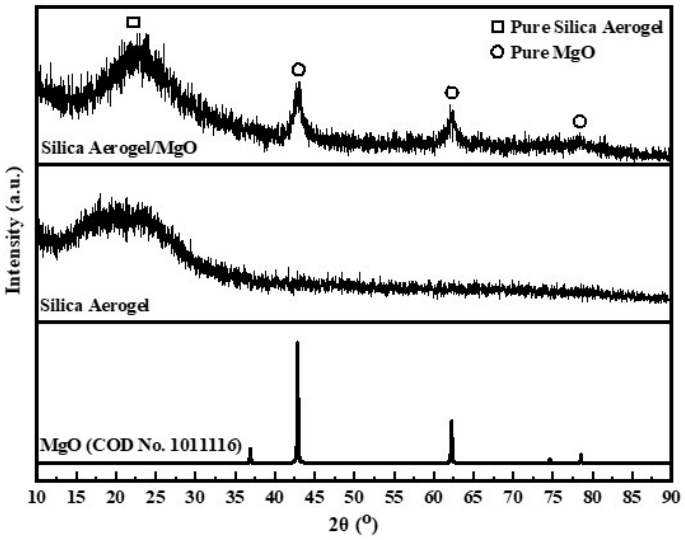

Figure 1. XRD Patterns of Silica Aerogel/MgO Composite, Silica Aerogel, and MgO

The XRD pattern of the silica aerogel/MgO composite is shown in Figure 1, while the corresponding characteristic peaks are listed in Table 2. The diffractogram shows that the composite contains both amorphous silica aerogel and crystalline MgO features. The broad diffraction band at around 15–30° 2θ confirms the amorphous nature of the silica framework. This amorphous structure is favorable for adsorption because it can provide accessible surface sites, pore volume, and pathways for adsorbate transport. Mahinroosta et al. (2024) also reported that amorphous silicate-based structures play an important role in providing adsorption sites for malachite green removal. In addition, the composite shows sharp diffraction peaks at 2θ values of 42.9°, 62.3°, and 78.6°, indicating the presence of MgO, which is consistent with the reference data (COD No. 1011116). The incorporation of MgO into the composite provides an important contribution by enhancing the surface basicity and introducing additional active sites, which may facilitate interactions with malachite green molecules during the adsorption process. The structural characteristics of the silica aerogel/MgO composite observed from XRD analysis were further confirmed by surface morphology analysis using SEM and surface area and pore size analysis using the BET method.

3.1.2 SEM (Scanning Electron Microscopy) and EDX (Energy -Dispersive X-ray) Mapping

The SEM images presented in Figure 2a-b show that pristine silica aerogel exhibits a porous and aggregated network structure, whereas the silica aerogel/MgO composite displays a rougher surface with visible particle agglomeration, indicating the deposition of MgO onto the silica matrix. Although agglomeration occurred, the porous structure was still maintained, allowing adsorbate diffusion toward the active sites. The elemental mapping results Figure 2c reveal that Si, O, and Mg were uniformly distributed and relatively homogeneously dispersed throughout the composite. The homogeneous distribution of Mg confirms that MgO was successfully integrated into the silica aerogel network, which may increase the number of surface active sites and enhance electrostatic interactions with malachite green molecules, as also reported by Ghoniem et al. (2022) and Hamad (2023). Furthermore, the EDX spectrum in Figure 2d further supports this result by showing dominant Si and O signals together with the presence of Mg. These morphological changes were further evaluated through BET analysis.

3.1.3 BET (Brunauer–Emmett–Teller) and BJH (Barrett–Joyner–Halenda)

The BET-BJH analysis showed that the silica aerogel/MgO composite had lower values than pristine silica aerogel, as shown in Table 3. This decrease indicates that MgO particles partially filled or blocked some pores, limiting nitrogen access during measurement. However, the average pore diameter increased, which may be attributed to pore restructuring after the modification process. The enlarged pores can support malachite green diffusion into the adsorbent interior, while MgO provides additional active sites for adsorption.

Figure 3 shows that both pristine silica aerogel and the

Table 2. XRD Peak of Silica Aerogel/MgO Composite

Sample	Main Features	Structure
Silica Aerogel	Broad peak (22°)	Amorphous
MgO	Sharp peak (36–75°)	Crystalline
Silica Aerogel/MgO	Combination of broad + sharp peaks	Amorphous-crystalline

Source: Azhar et al. (2025)

Table 3. Physical Properties of Silica Aerogel and Silica Aerogel/MgO

Parameter	Silica Aerogel	Silica Aerogel/MgO
BET Surface Area (m^2/g)	635.61	121.99
Pore Volume (cm^3/g)	0.97	0.50
BJH Desorption Average Pore Radius (nm)	2.799	6.517

Source: Azhar et al. (2025)

silica aerogel/MgO composite exhibited Type IV nitrogen adsorption-desorption isotherms with H3 hysteresis loops, confirming mesoporous characteristics and the presence of slit-like or interparticle pores Thommes et al. (2015). Pristine silica aerogel showed higher nitrogen uptake across the P/P_0 range, reflecting its larger surface area and pore volume. By contrast, the composite showed lower nitrogen adsorption capacity, most likely due to partial pore occupation by MgO. Nevertheless, the hysteresis loop remained visible, indicating that mesoporosity was retained after MgO incorporation. Since surface functional groups also affect adsorbent-adsorbate interactions, FTIR analysis was further conducted.

3.1.4 FTIR (Fourier Transform Infrared Spectroscopy)

Figure 4 illustrates the FTIR spectra of silica aerogel/ MgO composite before and after adsorption of malachite green, while the corresponding absorption bands are listed in Table 4. Prior to adsorption, several characteristic functional groups associated with potential adsorption sites were identified on composite surface. A broad absorption feature centered at 3435 cm^{-1} was assigned to the stretching vibration of hydroxyl groups originating from silanol functionalities and physically adsorbed water molecules. These surface hydroxyl groups are important because they can interact with malachite green through hydrogen bonding and may also contribute to the formation of negatively charged adsorption sites under appropriate pH conditions, thereby facilitating the uptake of the cationic dye. A weak signal observed at 2961 cm^{-1} was attributed to C–H stretching vibrations, which may be associated with residual species from surface modification process. The band located at 1635 cm^{-1} corresponded to the bending vibration of adsorbed water (H–O–H). In addition, the absorption bands at 1065 and 785 cm^{-1} were characteristic of Si–O–Si vibrations, confirming the silica aerogel framework. The presence of MgO within the composite was evidenced by the absorption band at 499 cm^{-1}, indicating successful incorporation and dispersion of MgO throughout the silica matrix.

Noticeable spectral change occurred after exposure to malachite green, suggesting the participation of surface functional groups in the adsorption process. The hydroxyl absorption band shifted from 3435 to 3345 cm^{-1} and exhibited increased broadening, implying that surface –OH groups were directly involved in interactions with dye molecules. Such changes are consistent with hydrogen-bond formation between hydroxyl groups on the adsorbent surface and nitrogen-containing functionalities present in malachite green, as well as possible interactions with the aromatic structure of the dye. Additional absorption bands emerged at 1533 and 1377 cm^{-1} following adsorption. These bands are associated with aromatic C=C and C–N vibrations characteristic of malachite green (You et al., 2022), providing direct evidence that dye molecules were successfully retained on the composite surface. Furthermore, the Mg–O vibration shifted from 499 to 492 cm^{-1} after adsorption, indicating the involvement of MgO-related active sites in the adsorption mechanism. This shift suggests that electrostatic interactions occurred between negatively charged oxygen-containing surface sites and positively charged malachite green molecules, thereby contributing to the overall adsorption process.

3.2 Effect of Adsorption Parameter Variations of Silica Aerogel/MgO on Malachite Green

Controlled adsorption data show a significant improvement after composite formation, where silica aerogel achieved only 22.1175 mg/g (19.66%), while the silica aerogel/MgO composite reached 96.9310 mg/g (86.1609%) under identical conditions. This marked enhancement highlights the role of MgO in strengthening adsorption interactions, supporting the existence of a synergistic effect between the porous silica structure and MgO active sites.

Based on this superior performance, further adsorption studies were focused on the silica aerogel/MgO composite to evaluate its behavior under various operational conditions. Adsorption capacity and removal percentage were used as the main indicators to evaluate the influence of these variables on adsorption behavior. The results are presented in Figures 5–7.

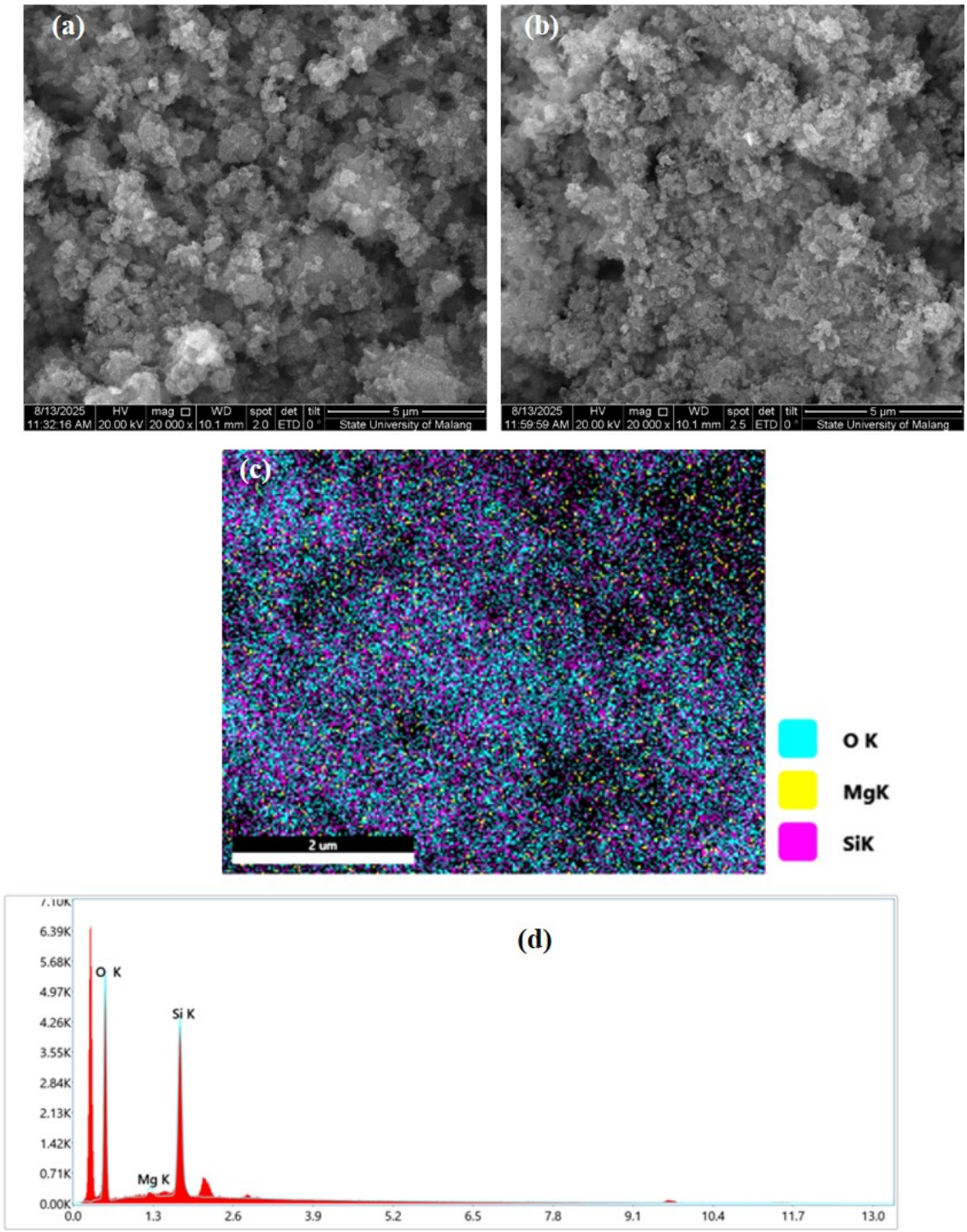

Figure 2. SEM of Silica Aerogel (a); SEM of Silica Aerogel/MgO Composite (b); and EDX Mapping for O, Mg, and Si (c). EDX Analysis for Point on the Surface of Silica Aerogel/MgO Composite (d)

3.2.1 Influence of Contact Time

Figure 5a–b shows how contact time affected adsorption capacity and removal efficiency. During the early stage, adsorption increased rapidly because many active sites were still available on the surface and inside the pores of the adsorbent. The high surface area and accessible porous structure supported the movement of dye molecules toward these sites. A clear increase in adsorption performance was observed from 30 to 80

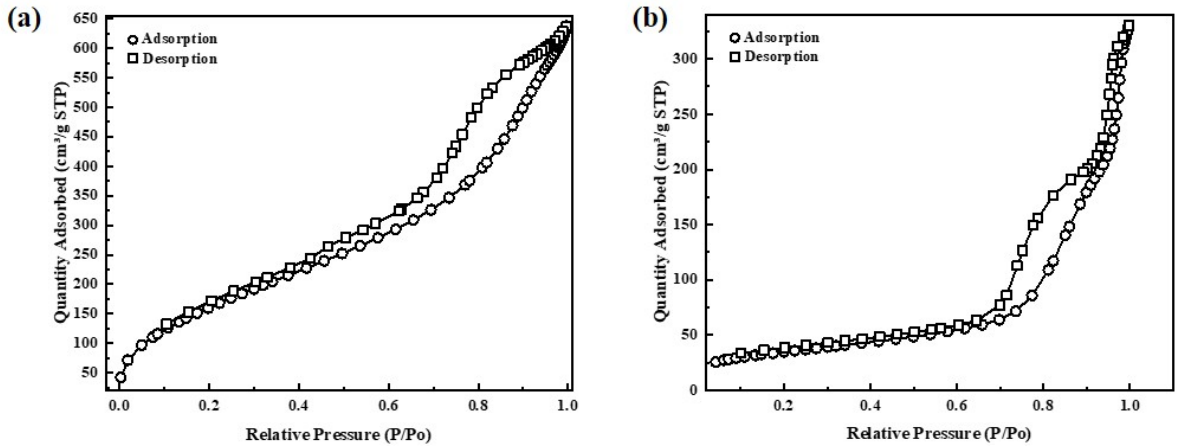

Figure 3. Adsorption-Desorption Curves of Silica Aerogel (a) and Silica Aerogel/MgO Composite (b)

Table 4. FTIR Absorption Bands of Silica Aerogel/MgO Composite

Wave Number (cm^{-1})			Functional Group
Silica Aerogel	Silica Aerogel/MgO	Silica Aerogel/MgO After Adsorption	
3437	3435	3345	O–H stretching (Si–OH, H_2O adsorbed)
2960	2960	2961	C–H (CH_3) stretching
1635	1635	1632	H–O–H bending (H_2O adsorbed)
–	–	1533	Aromatic C=C vibration and possible C–N vibration from malachite green
1439	1439	1377	C–H (CH_3) bending
1068	1065	1076	Si–O–Si asymmetric stretching
802	785	802	Si–C bending
–	499	492	Mg–O stretching

min. After this period, the adsorption rate decreased because the active sites became progressively occupied and repulsive interactions among adsorbed dye molecules increased. This behavior is typical for cationic dye adsorption, where the rate gradually declines as available sites become saturated (Obulapuram et al., 2021; Chouchane et al., 2023). After equilibrium was reached, the adsorption capacity and removal efficiency did not increase substantially. The equilibrium time was 80 min, with an adsorption capacity of 96.93 mg/g and a removal efficiency of 86.16%.

3.2.2 Influence of Adsorbent Dosage

The influence of adsorbent dosage was evaluated using 5–50 mg of silica aerogel/MgO composite. As shown in Figure 5c–d, the adsorption capacity increased from 75.02 mg/g at 5 mg to the maximum value of 96.90 mg/g at 10 mg, in contrast, the removal efficiency increased sharply at 10 mg and then remained relatively stable at higher adsorbent dosages. This enhancement occurred because increasing the adsorbent dose provided more surface area and active sites for dye binding. The porous morphology observed by SEM and the active functional groups identified by FTIR supported the interaction of malachite green with the adsorbent surface. However, when the dosage was increased beyond 10 mg, the adsorption capacity per unit mass decreased. This decline may be attributed to the distribution of a fixed amount of dye over a larger adsorbent mass, leaving many sites unused. Excess adsorbent may also promote particle clustering or overlapping of active sites, reducing the effective contact area and limiting mass transfer. Similar dosage-dependent behavior has been reported in previous dye adsorption studies (Mashkoor et al., 2018; Sen, 2023).

3.2.3 Influence of Initial Concentration

The effect of initial malachite green concentration was studied at 35–55 mg/L. Figure 6a shows that the adsorption capacity increased from 76.36 to 116.71 mg/g as the initial dye concentration increased. In contrast, Figure 6b indicates that the removal efficiency decreased from 87.27% to 84.88%. The higher adsorption capacity at greater dye concentration can be explained by the stronger concentration difference between the solution and adsorbent surface, which promotes mass transfer. At low dye concentration, the number of active sites was sufficient relative to the number of dye molecules, resulting in higher removal efficiency. At higher concentrations, however,

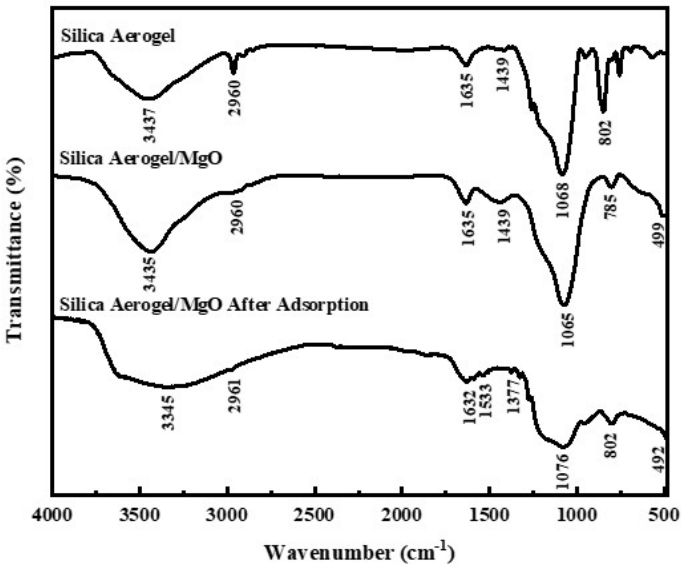

Figure 4. FTIR Spectra of Silica Aerogel, Silica Aerogel/Mgo, and Silica Aerogel/MgO After Adsorption

more active sites became occupied, and some dye molecules remained unadsorbed, causing a decrease in removal efficiency. This pattern agrees with general adsorption behavior, in which higher initial concentration increases uptake capacity but decreases removal percentage due to the limited number of available active sites (Sen, 2023; Li et al., 2022).

3.2.4 Influence of Temperature

The influence of temperature was examined at 25–45°C using malachite green concentrations of 35–55 mg/L. As presented in Figure 6c–d, adsorption capacity and removal efficiency increased with temperature under all tested conditions. This result indicates that the adsorption of malachite green was more favorable at higher temperature and followed an endothermic tendency. Higher temperature can increase the kinetic energy of malachite green molecules, accelerate their movement toward the adsorbent surface, and increase the frequency of collision with active sites. These conditions may enhance dye diffusion into the adsorbent pores and promote interactions with surface groups such as Si–OH and MgO-related sites. The observed behavior supports the endothermic nature of malachite green adsorption onto the silica aerogel/MgO composite (Budnyak et al., 2020; Hamad, 2023).

3.2.5 Influence of pH

Figure 7a shows that the pH_{PZC} of the adsorbent was 9, suggesting that the surface tends to be positively charged below pH 9 and negatively charged above pH 9. Although the pH_{PZC} occurred at pH 9, Figure 7b shows that adsorption capacity increased as the pH increased from acidic to near-alkaline conditions. In addition, Figure 7c shows that removal efficiency also improved with increasing pH, supporting stronger interaction between cationic malachite green molecules and progressively deprotonated active sites on the adsorbent surface. These trends indicate that adsorption was controlled not only by electrostatic attraction but also by the availability of active sites and the reduced competition of H^+ ions. Under acidic conditions, abundant H^+ ions can protonate surface hydroxyl groups such as Si–OH and Mg–OH, resulting in a more positively charged surface and weaker interaction with cationic malachite green. H^+ ions may also compete with dye molecules for the same adsorption sites. As pH increases, H^+ concentration decreases, lowering this competition. At the same time, surface hydroxyl groups may gradually undergo partial deprotonation to form negatively charged oxygen-containing sites, which can enhance electrostatic attraction toward malachite green. Therefore, although the pH_{PZC} was located at pH 9, surface deprotonation may occur gradually before the overall surface charge becomes negative. This explanation is supported by the FTIR spectra after adsorption, which showed shifts in the –OH and MgO-related bands, confirming the participation of surface hydroxyl groups and MgO active sites. Therefore, the higher adsorption capacity at elevated pH is associated with lower H^+ competition, greater contribution of negatively charged surface sites, and stronger interaction between malachite green and the active groups on the adsorbent surface (Raval et al., 2017).

3.2.6 Reusability of Silica Aerogel/MgO Composite

The reusability test shown in Figure 7d demonstrated that the silica aerogel/MgO adsorbent was able to maintain its adsorption performance after three cycles. In the first cycle, the removal efficiency was the highest because all active surface sites were still in optimal condition, and the active pores of the adsorbent were still open and accessible for interaction with the adsorbate. After regeneration and reuse in the second and third cycles, the removal efficiency decreased slightly. However, the decrease was relatively small, showing that the composite had acceptable stability and reusability.

Based on Figure 7d, the removal efficiency in the third cycle was slightly higher than that in the second cycle. This may occur because the regeneration process could remove residual dye molecules that previously covered some pores, allowing better access of the adsorbate to the active sites in the following cycle. However, since the difference was relatively small, this increase may still be within the range of experimental deviation and does not indicate a significant change. Overall, the reusability results show that the adsorbent has good stability and potential for repeated use without a sharp decrease in efficiency. The ability of an adsorbent to be regenerated and reused is an important factor in determining its sustainability for wastewater treatment applications.

3.3 Adsorption Equilibrium Parameters of Silica Aerogel/MgO toward Malachite Green

Adsorption equilibrium behavior was analyzed through kinetic modeling, equilibrium isotherms, and thermodynamic evaluation. Figure 8 presents the linearized plots of each model, which were used to determine the kinetic constants, isotherm

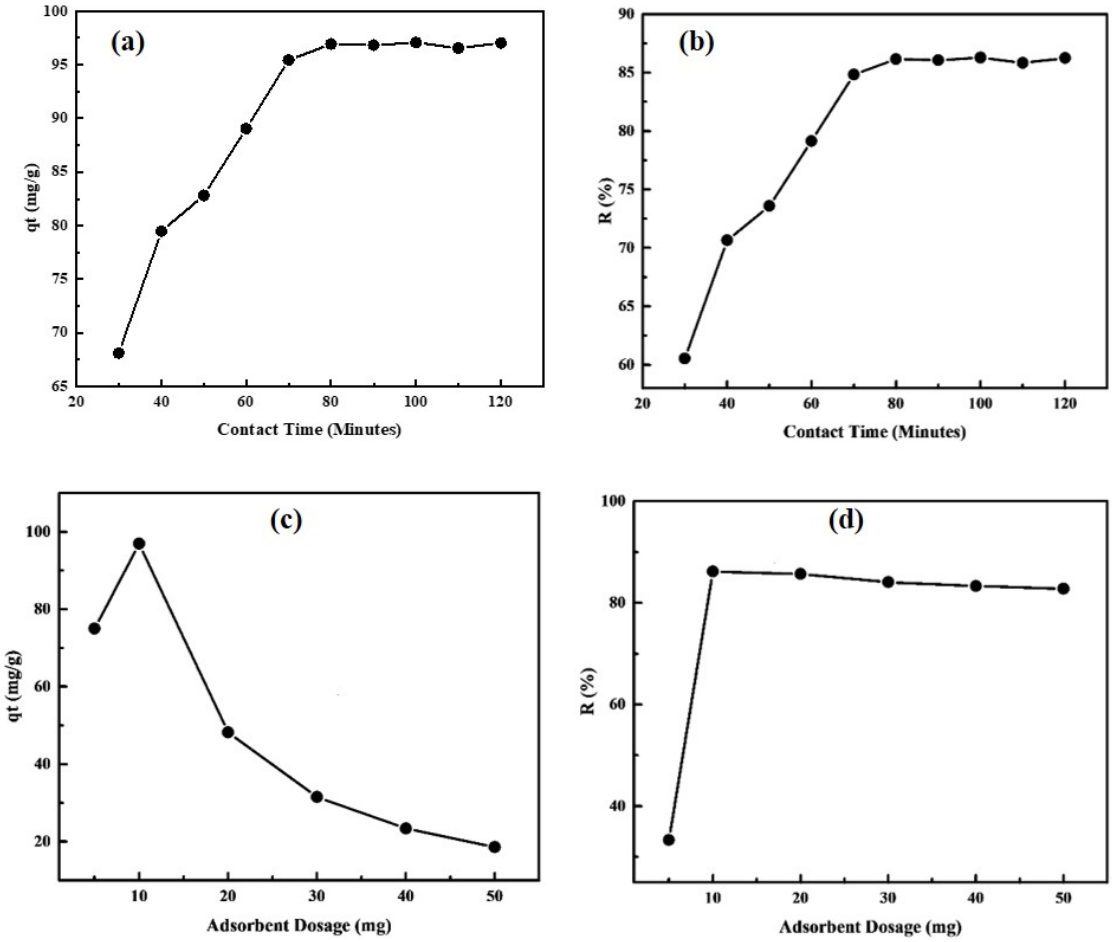

Figure 5. Effect of Contact Time on Adsorption Capacity (a); Effect of Contact Time on Removal Efficiency (b); Effect of Adsorbent Dosage on Adsorption Capacity (c); and Effect of Adsorbent Dosage on Removal Efficiency (d)

parameters, and thermodynamic energy values.

3.3.1 Adsorption Kinetics

The adsorption kinetic of malachite green onto the silica aerogel/MgO composite were evaluated using the pseudo-first-order and pseudo-second-order kinetic models. The corresponding fitting plots are presented in Figure 5a–b, while the kinetic parameters obtained from the models are summarized in Table 5. In adsorption systems, contact time plays a crucial role because it governs the duration available for adsorbate molecules to diffuse toward and interact with the active sites of the adsorbent. As illustrated in Figure 5a, dye adsorption capacity increased progressively with increasing contact time and reached equilibrium after approximately 80 min. The rapid uptake observed during the initial stage can be attributed to the abundance of unoccupied adsorption sites. As adsorption proceeded, the number of available sites gradually decreased, resulting in a slower adsorption rate until equilibrium was established.

A comparison of the kinetic models indicates that the pseudo-second-order equation provided a more satisfactory description of the experimental data than the pseudo-first-order model. As shown in Figure 8b and Table 5, the pseudo-second-order model yielded a higher coefficient of determination (R^2 = 0.9923), and the calculated equilibrium adsorption capacity (q_e) was in closer agreement with the experimentally measured value. In contrast, the pseudo-first-order model exhibited a considerably lower fitting quality, with an R^2 value of 0.8643. The superior performance of the pseudo-second-order model suggests that the adsorption process was influenced not only by transport of dye molecules from solution to the adsorbent surface but also by interactions occurring at active adsorption sites. Similar kinetic behavior has been reported for adsorption of dye molecules on metal oxide-containing adsorbents, where surface interactions significantly contribute to the overall adsorption mechanism (Hubbe et al., 2019). The kinetic findings are also consistent with FTIR results discussed previously. The observed shifts in the –OH and Mg–O vibration bands after adsorption indicate the participation of surface hydroxyl groups and MgO-related sites in the adsorption process. These active sites likely facilitate the retention of malachite green molecules through surface interactions, contributing to the excellent fit of

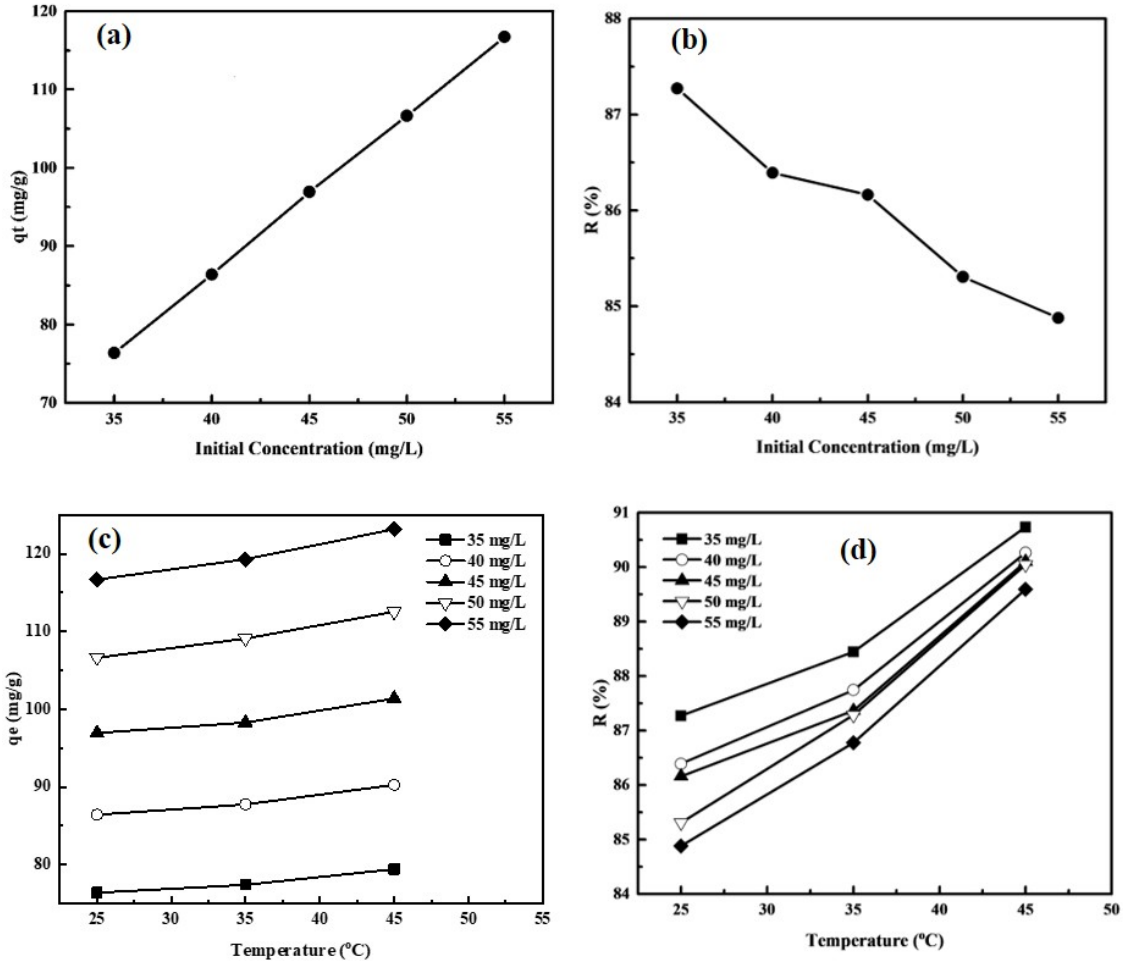

Figure 6. Effect of Initial Concentration on Adsorption Capacity (a); Effect of Initial Concentration on Removal Efficiency (b); Effect of Temperature on Adsorption Capacity (c); And Effect of Temperature on Removal Efficiency (d)

Table 5. Kinetic Parameters for Malachite Green Adsorption onto Silica Aerogel/MgO

Kinetic Parameter	Pseudo-First-Order	Pseudo-Second-Order
R^2	0.8643	0.9923
Rate constant	0.0672 (min^{-1})	0.0003 (g mg^{-1} min^{-1})
q_e calculated	277.1838 mg/g	132.1874 mg/g
q_e experimental	96.9310 mg/g	96.9310 mg/g

the pseudo-second-order model. Once equilibrium had been reached, the adsorption behavior was further evaluated using equilibrium isotherm models to investigate the distribution of malachite green molecules on the composite surface and to gain deeper insight into the adsorption mechanism.

3.3.2 Adsorption Isotherms

The equilibrium data were fitted using the Langmuir, Freundlich, and Temkin isotherm models to describe malachite green adsorption onto the silica aerogel/MgO composite. According to Figure 8c–e and Table 6, the Freundlich model showed the best agreement with the experimental data at all temperatures, with R^2 values of 0.9965–0.9973. These values were higher than those obtained from the Langmuir model, 0.9456–0.9841, and the Temkin model, 0.9888–0.9935. The Freundlich n values of 0.6824–0.7930 indicate that adsorption occurred on a heterogeneous surface and may involve multilayer coverage. The relatively good Temkin fit suggests that adsorbent–adsorbate interaction also contributed to dye uptake. Overall, the adsorption of malachite green onto the composite was not dominated by homogeneous monolayer coverage, but rather by heterogeneous surface interactions involving distributed active sites. This result agrees with previous studies on porous metal oxide-based composite adsorbents (Hamad,

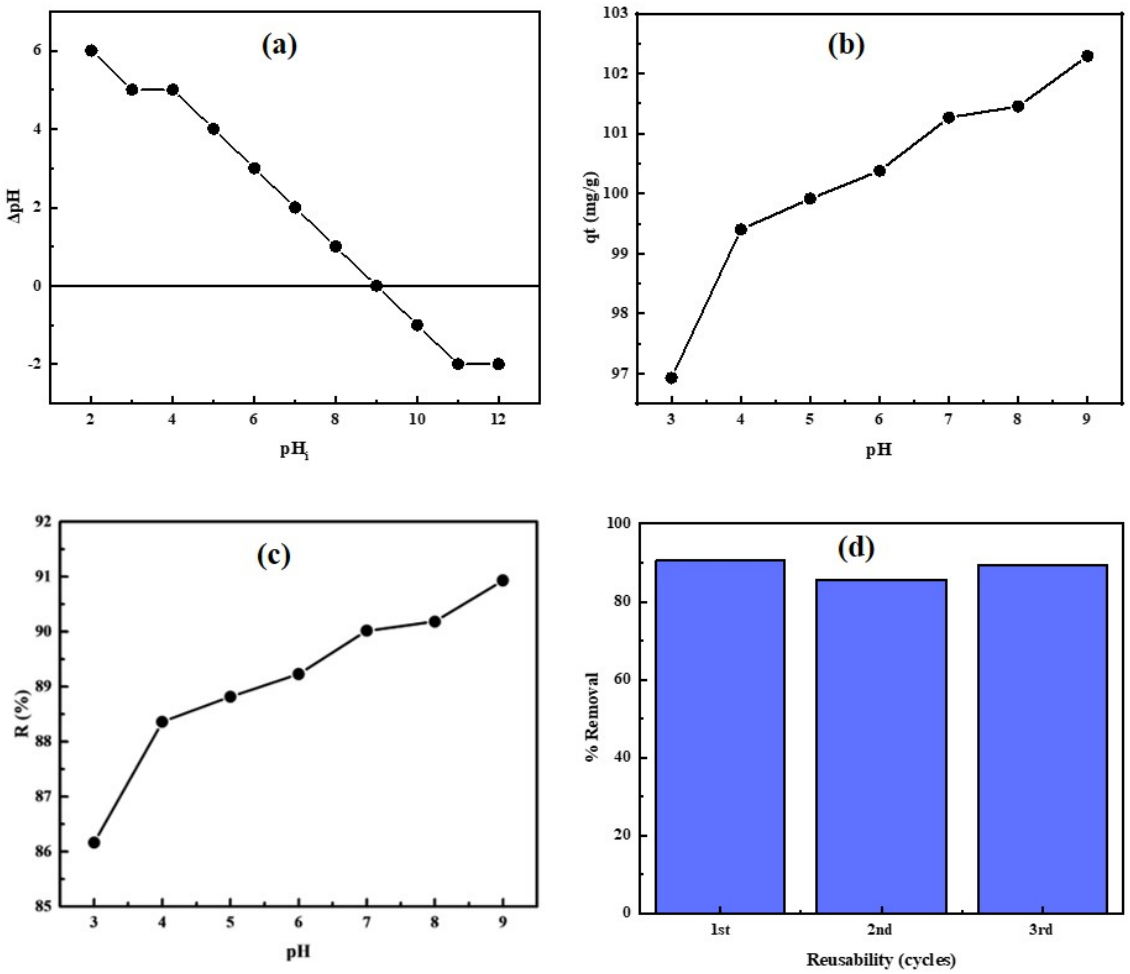

Figure 7. Determination of pH_{pzc}(a); Effect of pH on Adsorption Capacity (b); Effect of pH on Removal Efficiency (c); and Effect of Reusability of the Silica Aerogel/MgO Composite (d)

Table 6. Isotherm Parameters for Malachite Green Adsorption onto Silica Aerogel/MgO

Temperature	Langmuir Isotherm			Freundlich Isotherm			Temkin Isotherm	
	Q_L (mg/g)	K_L (L/mg)	R^2	K_F (L/mg)	n	R^2	b_T (J/mol)	R^2
25 °C	302.1148	0.0750	0.9841	27.4759	0.6824	0.9973	38.24	0.9935
35 °C	396.8254	0.0588	0.9540	26.8114	0.7525	0.9966	35.27	0.9888
45 °C	485.4369	0.0596	0.9456	31.0692	0.7930	0.9965	33.51	0.9917

Table 7. Thermodynamic Parameters for Malachite Green Adsorption onto Silica Aerogel/MgO

C_0 (mg/L)	$y = ax + b$	R^2	$\Delta G°$ (kJ/mol)			$\Delta H°$ (kJ/mol)	$\Delta S°$ (J/mol·K)
			25 °C	35 °C	45 °C		
35	7.0681–1498.5x	0.9430	-5.1069	-5.5258	-6.2897	12.4585	58.7642
40	7.2706–1578.9x	0.9473	-4.9412	-5.3750	-6.1577	13.1270	60.4478
45	7.2482–1578.5x	0.9253	-4.8998	-5.2970	-6.1141	13.1236	60.2615
50	8.0707–1839.0x	0.9726	-4.7513	-5.2809	-6.0996	15.2894	67.0998
55	7.7913–1764.5x	0.9680	-4.6802	-5.1809	-5.9822	14.6700	64.7769

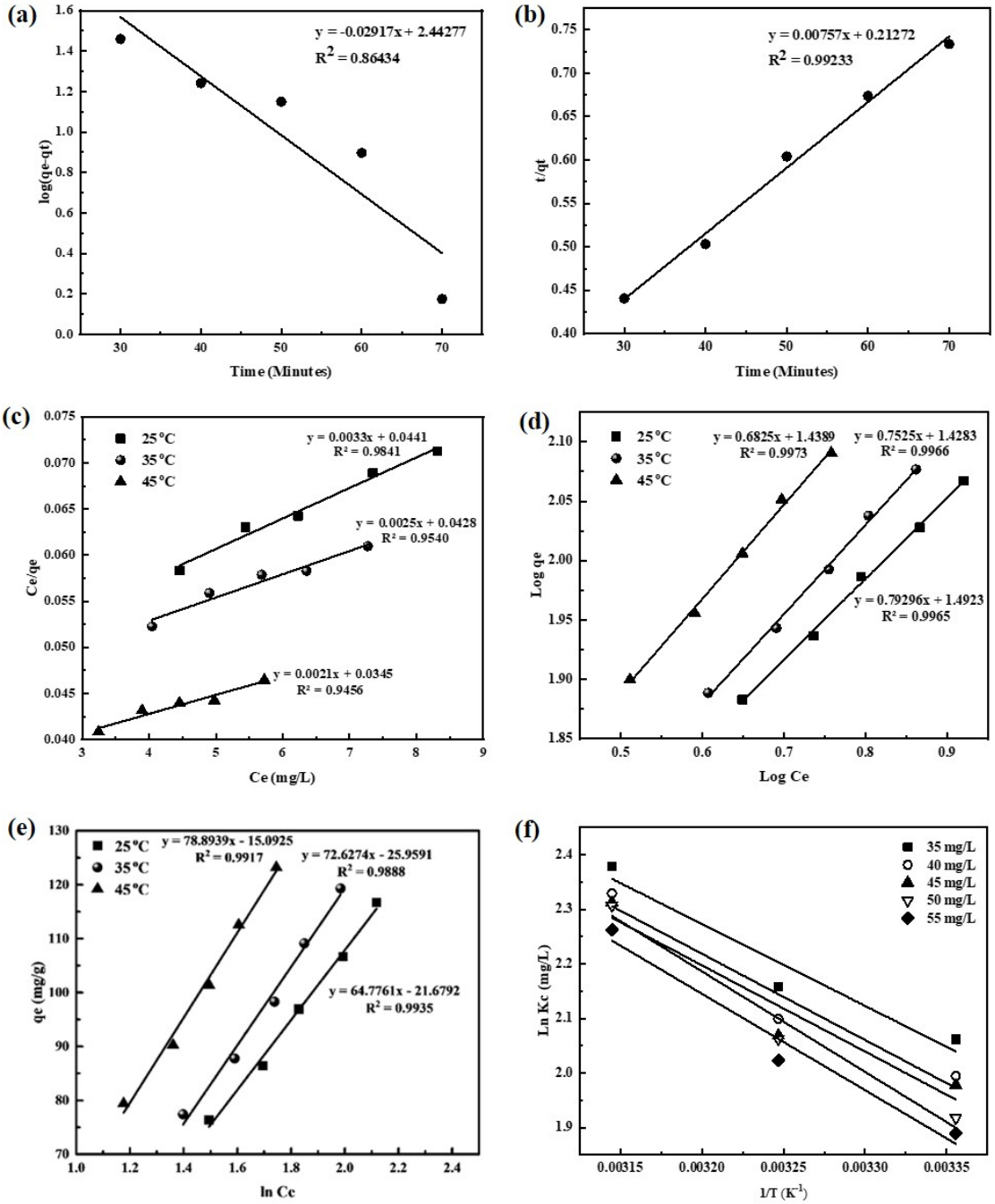

Figure 8. Linearized Plots of Pseudo-First-Order Kinetics (a), Pseudo-Second-Order Kinetics (b), Langmuir Isotherm (c), Freundlich Isotherm (d), Temkin Isotherm (e), and Van't Hoff Equation (f)

2023). Thermodynamic analysis was then carried out to evaluate the energetic behavior and spontaneity of adsorption.

3.3.3 Adsorption Thermodynamics

Thermodynamic parameters, including $\Delta G°$, $\Delta H°$, and $\Delta S°$, were calculated using the Van't Hoff equation at 25–45°C to evaluate the feasibility and energetic characteristics of malachite green adsorption onto the silica aerogel/MgO composite (Table 7). The Van't Hoff plot in Figure 8f and the data in Table 7 show that the process was spontaneous, endothermic, and accompanied by increased disorder at the solid–liquid interface. The negative $\Delta G°$ values of −4.68 to −6.29 kJ/mol confirm that adsorption was thermodynamically favorable at all temperatures. The positive $\Delta H°$ values of 12.46–15.29 kJ/mol

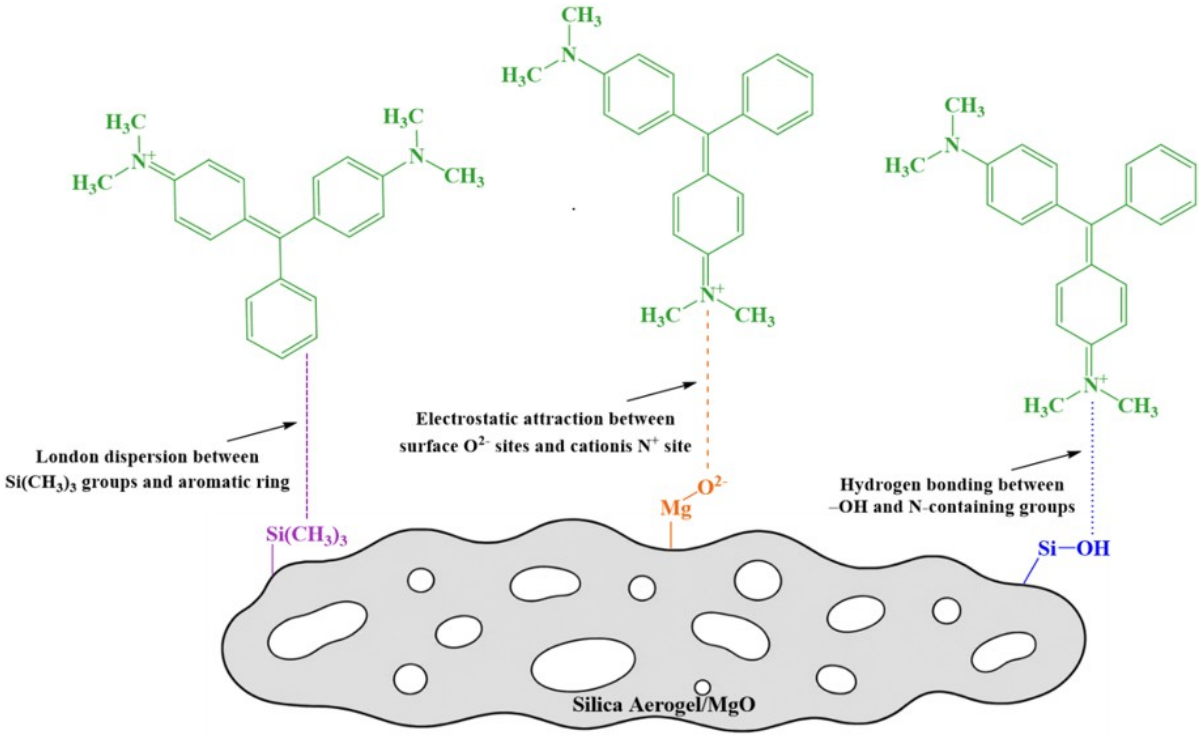

Figure 9. Proposed Adsorption Mechanism of Malachite Green Onto the Silica Aerogel/MgO Composite

Table 8. Comparative Adsorption Performance of the Present Silica Aerogel/MgO Composite and Previously Reported Open-Access Adsorbents for Malachite Green Removal

Adsorbent	Adsorption Capacity	Best Kinetic Model	Best Isotherm Model	Representative Operating Conditions	Source
Bagasse ash-derived silica aerogel/MgO composite (this work)	96.93 mg/g	Pseudo-second-order	Freundlich	80 min; 45 mg/L; 10 mg adsorbent; 25–45 °C; pH 3–9	Present work
Co_3O_4/MgO/$Mg_3B_2O_6$ nanocomposite (CBM600)	492.61 mg/g	Pseudo-second-order	Langmuir	70 min; 50–300 mg/L; 50 mg adsorbent; 25 °C; pH 10	Al-Wasidi et al. (2024)
Activated carbon from *Catha edulis* stem	5.62 mg/g	Pseudo-second-order	Freundlich	60 min; 10 mg/L; 500 mg adsorbent; room temperature; pH 10	Abate et al. (2020)
Ni/Al layered double hydroxide-graphene oxide composite	111.11 mg/g	Pseudo-second-order	Langmuir	20 mg adsorbent; optimum pH 4; temperature and concentration varied	Amri et al. (2023)
TiO_2/f-MWCNT nanocomposite	38.61 mg/g	Pseudo-second-order	Langmuir-2	10 min; 5 mg adsorbent; 20 °C; pH 8	Jomardani et al. (2026)

indicate an endothermic process, meaning that higher temperature promoted dye interaction with the adsorbent surface. This result is consistent with the higher adsorption capacity observed at elevated temperature. The positive $\Delta S°$ values of 58.76–67.10 J/mol·K indicate increased randomness during adsorption. Based on the relatively low $\Delta G°$ magnitude, below 20 kJ/mol, together with positive $\Delta H°$ and $\Delta S°$, the process is likely dominated by physisorption, while electro-

static interactions also contribute between cationic malachite green and negatively charged/basic MgO sites in the composite (Chakraborty et al., 2021; Gaur et al., 2024).

To further position the performance of the present silica aerogel/MgO composite within the existing literature, Table 8 compares the present material with several previously reported open-access adsorbents for malachite green removal. This comparison highlights the relative adsorption performance, modeling behavior, and operating conditions of the present material.

3.3.4 Adsorption Mechanism

The combined characterization and adsorption results provide a basis for understanding the adsorption mechanism of malachite green onto the silica aerogel/MgO composite. The amorphous structure and porous network of the silica aerogel/MgO composite, as confirmed by XRD, SEM, and BET analyses, provide sufficient contact area and diffusion pathways for malachite green molecules. FTIR analysis identified hydroxyl groups and MgO-related active sites, which served as important interaction centers during adsorption. The pH and pH_{PZC} results further indicated that electrostatic attraction between the negatively charged adsorbent surface and cationic malachite green was the main driving interaction. The pseudo-second-order kinetic fit, together with the thermodynamic results, suggests that adsorption involved physical adsorption accompanied by stronger surface interactions, especially electrostatic attraction. Therefore, the adsorption performance of the silica aerogel/MgO composite can be attributed to the combined effects of its textural properties and surface chemistry. Figure 9 illustrates the proposed mechanism, including electrostatic attraction, hydrogen bonding, and possible secondary interactions between malachite green molecules and the active sites of the composite.

4. CONCLUSION

A biomassa-derived silica aerogel/MgO composite was successfully developed and demonstrated effective performance for the removal malachite green from aqueous solution. The combined characterization results revealed that the incorporation of MgO into the porous silica aerogel framework generated a mesoporous adsorbent containing abundant hydroxyl groups and accessible active sites. The integration of structural, surface, and adsorption analyses indicates that enhanced adsorption performance originated from the synergistic contribution of the silica aerogel network and dispersed MgO particles. The adsorption behavior was strongly influenced by solution pH, contact time, adsorbent dosage, initial dye concentration, and temperature. The increase in adsorption capacity under alkaline conditions, together with FTIR band shifts observed after adsorption, suggests that surface hydroxyl groups and MgO-related sites played important roles in dye binding. The kinetic, equilibrium, and thermodynamic result consistently indicate that adsorption occurred on energetically heterogeneous surfaces through multiple interaction pathways, including electrostatic attraction, hydrogen bonding, and pore-assisted diffusion. Under the optimum operating conditions, the composite achieved an adsorption capacity of 123.19 mg/g and a removal efficiency of 90.93%, substantially outperforming pristine silica aerogel. These results highlight the beneficial role of MgO incorporation in improving the adsorption capability of the silica aerogel matrix. Overall, the findings demonstrate that bagasse can be converted into a value-added adsorbent with promising potential for wastewater treatment applications. The combinations of a renewable silica source and MgO active sites provided an environmentally friendly strategy for developing efficient adsorbents for cationic dye removal.

5. ACKNOWLEDGMENT

The authors express their sincere appreciation to Universitas Negeri Malang for supporting this work through its non-APBN funding program.

REFERENCES

Abate, G. Y., A. N. Alene, A. T. Habte, and D. M. Getahun (2020). Adsorptive Removal of Malachite Green Dye from Aqueous Solution onto Activated Carbon of Catha edulis Stem as a Low-Cost Bio-Adsorbent. *Environmental Systems Research*, **9**(1); 29

Abu Elella, M. H., E. S. Goda, H. Gamal, S. M. El-Bahy, M. A. Nour, and K. R. Yoon (2021). Green Antimicrobial Adsorbent Containing Grafted Xanthan Gum/ SiO_2 Nanocomposites for Malachite Green Dye. *International Journal of Biological Macromolecules*, **191**; 385–395

Agustina, Y., Hamidah, and Nazriati (2022). Reducing Textile Dyes from Liquid Waste Using ZnO/Silica Aerogel Nanocomposites. In *AIP Conference Proceedings*, volume 2638. page 100007

Akram, M., R. Rehman, G. Samin, Z. T. Al-Thagafi, M. E. Al-Hazemi, and E. A. Al-Abbad (2023). Decontamination of Malachite Green and Victoria Blue-B Dyes by High-Speed Photo-Catalyzer Reactor Using Titania and Zinc Oxide as Catalysts. *Journal of Water Process Engineering*, **53**; 103757

Al-Wasidi, A. S., E. A. Abdelrahman, R. K. Shah, N. A. Abdelhakim, and F. A. Saad (2024). Facile Synthesis of Novel Nanocomposite Composed of Co_3O_4, MgO, and $Mg_3B_2O_6$ for Malachite Green Dye Decontamination from Aqueous Media. *Scientific Reports*, **14**(1); 30570

Amri, A., A. Lesbani, and R. Mohadi (2023). Malachite Green Dye Adsorption from Aqueous Solution Using a Ni/Al Layered Double Hydroxide-Graphene Oxide Composite Material. *Science and Technology Indonesia*, **8**(2); 280–287

Azhar, I. M., N. Nazriati, and I. K. Kusumaningrum (2025). Utilization of Bagasse Ash for the Preparation of Silica Aerogel/MgO Composites Through Ambient-Pressure Drying. *Walisongo Journal of Chemistry*, **8**(2); 251–258

Benjelloun, M., Y. Miyah, G. A. Evrendilek, F. Zerrouq, and S. Lairini (2021). Recent Advances in Adsorption Kinetic

Models: Their Application to Dye Types. *Arabian Journal of Chemistry*, **14**(4); 103031

Budnyak, T. M., M. Błachnio, A. Slabon, A. Jaworski, V. A. Tertykh, A. Deryło-Marczewska, and A. W. Marczewski (2020). Chitosan Deposited onto Fumed Silica Surface as Sustainable Hybrid Biosorbent for Acid Orange 8 Dye Capture: Effect of Temperature in Adsorption Equilibrium and Kinetics. *The Journal of Physical Chemistry C*, **124**(28); 15312–15323

Chakraborty, S., A. Mukherjee, S. Das, N. R. Maddela, S. Iram, and P. Das (2021). Study on Isotherm, Kinetics, and Thermodynamics of Adsorption of Crystal Violet Dye by Calcium Oxide Modified Fly Ash. *Environmental Engineering Research*, **26**(1); 190372

Chouchane, T., A. Boukari, O. Khireddine, S. Chibani, and S. Chouchane (2023). Equilibrium, Kinetics, and Thermodynamics of Batch Adsorption of Mn(II) Ions on Blast Furnace Slag (BFS) and Kaolin (KGA). *Journal of Engineering and Applied Science*, **70**; 58

Foo, K. Y. and B. H. Hameed (2010). Insights into the Modeling of Adsorption Isotherm Systems. *Chemical Engineering Journal*, **156**(1); 2–10

Gaur, B., J. Mittal, H. Hassan, A. Mittal, and R. T. Baker (2024). Ordered Mesoporous Carbon as Adsorbent for the Removal of a Triphenylmethane Dye from Its Aqueous Solutions. *Molecules*, **29**(17); 4100

Ghoniem, M. G., F. A. M. Ali, B. Y. Abdulkhair, M. R. A. Elamin, A. M. Alqahtani, S. Rahali, and M. A. Ben Aissa (2022). Highly Selective Removal of Cationic Dyes from Wastewater by MgO Nanorods. *Nanomaterials*, **12**(6); 1023

Gui, C. X., Q. J. Li, L. L. Lv, J. Qu, Q. Q. Wang, S. M. Hao, and Z. Z. Yu (2015). Core–Shell Structured MgO@Mesoporous Silica Spheres for Enhanced Adsorption of Methylene Blue and Lead Ions. *RSC Advances*, **5**(26); 20440–20445

Hamad, M. T. M. H. (2023). Optimization Study of the Adsorption of Malachite Green Removal by MgO Nano-Composite, Nano-Bentonite and Fungal Immobilization on Active Carbon Using Response Surface Methodology and Kinetic Study. *Environmental Sciences Europe*, **35**(1); 1–37

Hubbe, M. A., S. Azizian, and S. Douven (2019). Implications of Apparent Pseudo-Second-Order Adsorption Kinetics onto Cellulosic Materials: A Review. *BioResources*, **14**(3); 7582–7626

Jomardani, F., R. Shakeri, R. Akbarzadeh, and S. N. Kokhdan (2026). Adsorption Kinetics and Isotherms of Malachite Green Removal from Aqueous Solution Using TiO2-Loaded on f-MWCNTs Nanocomposite. *Scientific Reports*, **16**(1); 8567

Li, J., X. Dong, X. Liu, X. Xu, W. Duan, J. Park, and Y. Lu (2022). Comparative Study on the Adsorption Characteristics of Heavy Metal Ions by Activated Carbon and Selected Natural Adsorbents. *Sustainability*, **14**(23); 15579

Liu, X., Y. Wu, W. Zhao, Z. Wu, H. Han, Z. Xie, and T. H. Ko (2023). Adsorption of Malachite Green from Aqueous Phase by Tea Stalk Powder: Parameters, Kinetic, Isothermal, and Thermodynamic Studies. *BioResources*, **18**(3); 6364–6383

Mahinroosta, M., R. M. Moattari, A. Allahverdi, and P. Ghadir (2024). Malachite Green Dye Removal with Aluminosilicate Nanopowder from Aluminum Dross and Silicomanganese Slag. *Circular Economy*, **3**(3); 100100

Mashkoor, F., A. Nasar, Inamuddin, and A. M. Asiri (2018). Exploring the Reusability of Synthetically Contaminated Wastewater Containing Crystal Violet Dye Using Tectona grandis Sawdust as a Very Low-Cost Adsorbent. *Scientific Reports*, **8**; 8314

Murphy, O. P., M. Vashishtha, P. Palanisamy, and K. V. Kumar (2023). A Review on the Adsorption Isotherms and Design Calculations for the Optimization of Adsorbent Mass and Contact Time. *ACS Omega*, **8**(20); 17407–17430

Nazriati, N., H. Setyawan, S. Affandi, M. Yuwana, and S. Winardi (2014). Using Bagasse Ash as a Silica Source When Preparing Silica Aerogels via Ambient Pressure Drying. *Journal of Non-Crystalline Solids*, **400**; 6–11

Obulapuram, P. K., T. Arfin, F. Mohammad, S. K. Khiste, M. Chavali, A. N. Albalawi, and H. A. Al-Lohedan (2021). Adsorption, Equilibrium Isotherm, and Thermodynamic Studies Towards the Removal of Reactive Orange 16 Dye Using Cu(I)-Polyaniline Composite. *Polymers*, **13**(20); 3490

Pandey, S., J. Y. Do, J. Kim, and M. Kang (2020). Fast and Highly Efficient Catalytic Degradation of Dyes Using κ-Carrageenan Stabilized Silver Nanoparticles Nanocatalyst. *Carbohydrate Polymers*, **230**; 115597

Raval, N. P., P. U. Shah, and N. K. Shah (2016). Nanoparticles Loaded Biopolymer as Effective Adsorbent for Adsorptive Removal of Malachite Green from Aqueous Solution. *Water Conservation Science and Engineering*, **1**; 69–81

Raval, N. P., P. U. Shah, and N. K. Shah (2017). Malachite Green: A Cationic Dye and Its Removal from Aqueous Solution by Adsorption. *Applied Water Science*, **7**; 3407–3445

Sen, T. K. (2023). Agricultural Solid Wastes Based Adsorbent Materials in the Remediation of Heavy Metal Ions from Water and Wastewater by Adsorption: A Review. *Molecules*, **28**(14); 5575

Shoaib, A. G., S. Ragab, A. El Sikaily, M. Yılmaz, and A. El Nemr (2023). Thermodynamic, Kinetic, and Isotherm Studies of Direct Blue 86 Dye Adsorption by Cellulose Hydrogel. *Scientific Reports*, **13**; 5910

Tarekegn, M. M., R. M. Balakrishnan, A. M. Hiruy, and A. H. Dekebo (2021). Removal of Methylene Blue Dye Using Nano Zerovalent Iron, Nanoclay and Iron Impregnated Nanoclay: A Comparative Study. *RSC Advances*, **11**(48); 30109–30131

Thommes, M., K. Kaneko, A. V. Neimark, J. P. Olivier, F. Rodriguez-Reinoso, J. Rouquerol, and K. S. W. Sing (2015). Physisorption of Gases, with Special Reference to the Evaluation of Surface Area and Pore Size Distribution (IUPAC Technical Report). *Pure and Applied Chemistry*, **87**(9–10); 1051–1069

Umeh, C. T., A. B. Akinyele, N. H. Okoye, S. S. Emmanuel,

K. O. Iwuozor, I. P. Oyekunle, J. O. Ocheje, and J. O. Ighalo (2023). Recent Approach in the Application of Nanoadsorbents for Malachite Green (MG) Dye Uptake from Contaminated Water: A Critical Review. *Environmental Nanotechnology, Monitoring & Management*, **20**; 100891

Wang, M., Y. Jiao, N. Li, and Y. Su (2023). Synthesis of a SiO_2-MgO Composite Material Derived from Yellow Phosphorus Slag with Excellent Malachite Green Adsorption Activity. *Journal of Alloys and Compounds*, **969**; 172344

You, X., R. Zhou, Y. Zhu, D. Bu, and D. Cheng (2022). Adsorption of Dyes Methyl Violet and Malachite Green from Aqueous Solution on Multi-Step Modified Rice Husk Powder in Single and Binary Systems: Characterization, Adsorption Behavior and Physical Interpretations. *Journal of Hazardous Materials*, **430**; 128445

